

Ionothermal Synthesis of Sulfidobismuth *spiro*-Dicubane Cations

Maximilian Knies^[a] and Michael Ruck^{*[a, b]}

Dedicated to Professor Johannes Beck on the Occasion of his 65th Birthday.

Bi_2S_3 was dissolved in the presence of NaCl in the ionic liquid [BMIm]Cl·4AlCl₃ (BMIm = 1-*n*-butyl-3-methylimidazolium) through annealing the mixture at 180 °C. Upon cooling to room temperature, orange, air-sensitive crystals of Na(Bi₇S₈)[S-

(AlCl₃)₃][AlCl₄]₂ (**1**) precipitated. X-ray diffraction on single-crystals of **1** revealed a triclinic crystal structure that contains (Bi₇S₈)⁵⁺ *spiro*-dicubanes, [S(AlCl₃)₃]²⁻ tetrahedra triples, isolated [AlCl₄]⁻ tetrahedra, and sodium cations.

1. Introduction

The use of ionic liquids (ILs)^[1] as solvents in inorganic synthesis is becoming increasingly popular as they make materials accessible at low temperatures and in high purity or open paths to new compounds that cannot be synthesized by conventional methods.^[2–13] Some ILs are able to dissolve inorganic compounds that are conventionally hardly soluble without harsh conditions.^[14,15] One example is bismuth(III) sulfide, Bi₂S₃, also known as the mineral bismuthinite, which usually requires conditions such as hot nitric acid to be dissolved but readily does so in ILs.^[16–18] The formation of complex ionic species seems to be facilitated in ILs through incorporation of and stabilization through weakly coordinating anions, originating from the solvent itself.^[6,10,13] Thus, contrary to most other solvents, ILs cannot always be regarded as inert reaction media.^[19–21]

Salts containing cations composed of pnictogen and chalcogen atoms are comparatively rare. In 1975, Gillespie et al. reported the first cationic sulfidonitrogen rings.^[22–24] The up to now solitary binary cation containing phosphorous, the polyhedral (P₃Se₄)⁺, was discovered only recently.^[25] For the semi-metallic elements of group 15, the isostructural cages (As₃Ch₄)⁺ (Ch = S, Se) are known.^[26,27] The sulfur-containing cation also occurs with a capping atom as (As₃S₅)⁺.^[27] Reactions with tellurium led to the trigonal prism (As₂Te₄)²⁺.^[28] Antimony-based pnictogen-chalcogen polycations exist in great variety of shapes and sizes, e.g. the (Sb₂Te₄)²⁺ prism,^[28] the capped trigonal prism

(Sb₃Te₄)³⁺,^[28] the cubes (Sb₄Ch₄)⁴⁺^[28] or the *spiro*-dicubanes (Sb₇Ch₈)⁵⁺ with Ch = S, Se, Te. The latter crystallized without^[29,30] or together with other metal cations,^[30,31] or as (Sb₇Ch₈X₂)³⁺ with terminal halogen atoms (X = Cl, Br).^[30,32,33] Furthermore, *spiro*-tetracubanes [Sb₁₃Se₁₆Br₂]⁵⁺,^[32] linked realgar cages [Sb₁₀Se₁₀]¹²⁺,^[34] and periodic *catena*-polycations^[35,36] were isolated.

Cuboid shapes are also dominating among the bismuth-chalcogen cations. Beck et al. crystallized (Bi₄S₄)⁴⁺, the first binary sulfidobismuth(III) polycation, from a NaAlCl₄ flux.^[37] Heterocubanes were also observed for the heavier chalcogen homologues in (Bi₄Ch₄)[TrCl₄]₄ (Ch = Se, Te, Tr = Al, Ga).^[28,37,38] Substitution of one bismuth vertex with an Al–Cl^[17] or a Ga–S^[39] dumbbell as well as extension to a *spiro*-dicubane^[18] were observed so far. We recently discovered the double salt [BMIm](Bi₄S₄)[AlCl₄]₅ (BMIm = 1-*n*-butyl-3-methylimidazolium), which incorporates the reaction medium [BMIm][AlCl₄] and precipitates only in the presence of metal cations like gold(I) or platinum(II).^[18]

The incorporation of metal cations alongside *spiro*-dicubane polycations has particularly been observed for the isostructural telluridoantimony(III) compounds M(Sb₇Te₈)[TrCl₄]₆ (M = Ag, Cu, Na; Tr = Al, Ga).^[29–31] The sodium and silver compounds undergo phase transitions between 177 K and 93 K, which leads to splitting of the monovalent metal cation positions accompanied by a doubling of the lattice parameter *c*.^[29,30] Besides, only the recently discovered Ag(Bi₇S₈)[S(AlCl₃)₃]₂[AlCl₄]₂ contains binary pnictogen-chalcogen cations alongside metal ions.^[18] Its triclinic crystal structure is a stack of layer packages with trigonal layer symmetry. The pseudosymmetry is induced by the molecular symmetry of the *spiro*-dicubane and the [S(AlCl₃)₃]²⁻ anion. It provides numerous positions of similar energy for the silver cations, which results in extended disorder that persists even upon slow cooling of the crystals.

Herein, we report on the IL-based synthesis and crystal structure of a new sulfidobismuth(III) compound, incorporating alkali metal ions, Na(Bi₇S₈)[S(AlCl₃)₃]₂[AlCl₄]₂ (**1**) as well as experimental indications of similar compounds containing potassium, rubidium, or cesium.

[a] M. Knies, Prof. Dr. M. Ruck
Faculty of Chemistry and Food Chemistry
Technische Universität Dresden
01069 Dresden (Germany)
E-mail: michael.ruck@tu-dresden.de

[b] Prof. Dr. M. Ruck
Max Planck Institute for Chemical Physics of Solids
Nöthnitzer Str. 40
01187 Dresden (Germany)

Supporting information for this article is available on the WWW under <https://doi.org/10.1002/open.202100145>

© 2021 The Authors. Published by Wiley-VCH GmbH. This is an open access article under the terms of the Creative Commons Attribution License, which permits use, distribution and reproduction in any medium, provided the original work is properly cited.

2. Results and Discussion

2.1. Synthesis Results and Substitution Attempts

A mixture of NaCl and Bi₂S₃ in the molar ratio of 2:1 was dissolved in the ionic liquid [BMIm]Cl·4AlCl₃ at 180 °C. Upon cooling to room temperature, deep red, shiny crystals of Na(Bi₇S₈)[S(AlCl₃)₃]₂[AlCl₄]₂ (1) crystallized alongside minor amounts of [BMIm](Bi₄S₄)[AlCl₄]₅^[18] and solidified AlCl₃ (Figure S1, Supporting Information). Energy dispersive X-ray spectroscopy (EDX) confirmed the composition, particularly the presence of sodium in 1.

Analogous syntheses using the chlorides of other alkali metals ($M=K, Rb, Cs$) yielded crystals of similar color, shape and composition, according to EDX measurements. X-ray diffraction experiments on these crystals showed a high degree of diffuse scattering on the reflection rows parallel the b^* axis, as well as low Bragg intensities. We suppose stacking faults to cause these effects, which also affect the crystal structure of 1 but to a lesser extent. Although a full crystal structure analysis was impossible, at least approximate lattice parameters for the compounds with $M=K, Cs$ could be determined (Table 1). These unit cells resemble the one of Ag(Bi₇S₈)[S(AlCl₃)₃]₂[AlCl₄]₂^[18] strongly suggesting compounds $M(Bi_7S_8)[S(AlCl_3)_3]_2[AlCl_4]_2$ with analogous layered structures.

2.2. Crystal Structure of Na(Bi₇S₈)[S(AlCl₃)₃]₂[AlCl₄]₂

Sodium(I)-*spiro*[8,8]sulfidobismuth(III)cubane-bis{tris{trichloridoaluminate(III)}sulfide}-bis{tetrachloridoaluminate(III)},

1, crystallizes in the triclinic space group $P\bar{1}$ (no. 2) with two formula unit per unit cell and the lattice parameters $a=1846.4(2)$ pm, $b=1905.1(2)$ pm, $c=1065.5(1)$ pm, $\alpha=84.07(1)^\circ$, $\beta=89.55(1)^\circ$, $\gamma=49.68(1)^\circ$ and $V=2833.9(4)$ 10⁶ pm³ at 100(2) K. Atomic parameters and interatomic distances are listed in Tables S1 and S2 of the Supporting Information. The crystal structure (Figure 1) features three different complex ions, (Bi₇S₈)⁵⁺ *spiro*-dicubane cations, [S(AlCl₃)₃]²⁻ anions and [AlCl₄]⁻ tetrahedra, as well as sodium(I) cations (Figure 2).

The structure of 1 is composed of layer packages ($d \approx 1160$ pm), which resemble those in Ag(Bi₇S₈)[S(AlCl₃)₃]₂[AlCl₄]₂ (2)^[18] and Na⁺ cations in the inter-layer space ($d \approx 260$ pm). While the silver compound 2 has a high layer symmetry that

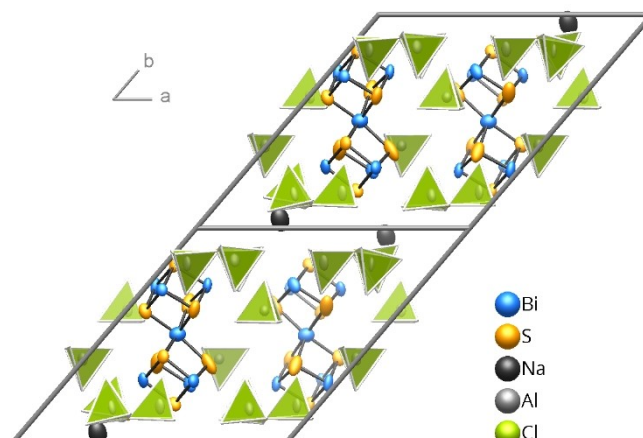


Figure 1. Crystal structure of 1 at 100(2) K. [S(AlCl₃)₃]²⁻ and [AlCl₄]⁻ anions are depicted as Al-centered polyhedra. The ellipsoids comprise 99% of the probability density of the atoms.

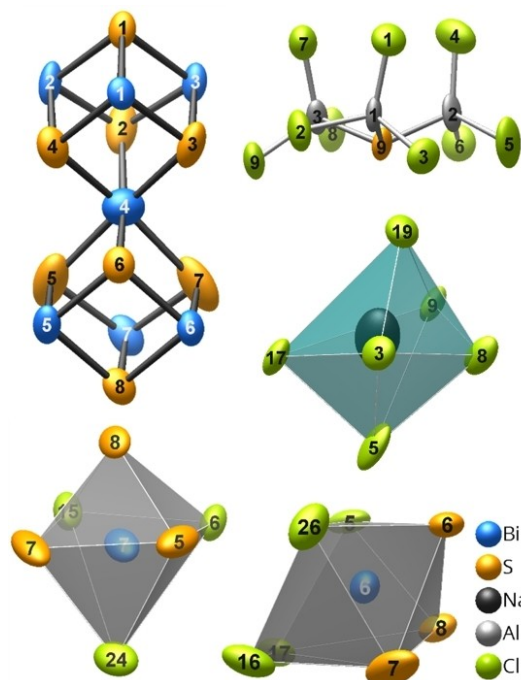


Figure 2. (Bi₇S₈)⁵⁺ *spiro*-dicubane cation, [S(AlCl₃)₃]²⁻ anion, and coordination polyhedra of the sodium(I) cation and bismuth(III) atoms in 1. The ellipsoids comprise 99% of probability density of atoms at 100(2) K.

Table 1. Lattice parameters of compounds $M(Bi_7S_8)[S(AlCl_3)_3]_2[AlCl_4]_2$ with $M=Ag, K, Cs$ at room temperature.			
M	Ag ^[16]	K	Cs
a/pm	1064.5(1)	1052(18)	1068(2)
b/pm	1067.0(1)	1061(20)	1068(2)
c/pm	1513.3(1)	1560(20)	1608(3)
$\alpha/^\circ$	77.17(1)	77.8(4)	70.7(1)
$\beta/^\circ$	75.59(1)	70.8(4)	74.4(1)
$\gamma/^\circ$	60.42(1)	61.2(4)	60.1(1)
$V/(10^6 \text{ pm}^3)$	1437.7(1)	1438(8)	1488(1)

was reduced to $P\bar{1}$ through stacking, in the sodium compound 1, the molecular units themselves are distorted and the deviations from the layer group $\bar{p}3m1$ (no. 72)^[40] are larger than in 2. This goes hand in hand with an ordered distribution of the

monovalent cations in **1** and seems to be associated with the size and the polarizability of the M^+ cation. Among the discussed monovalent cations, Na^+ is the smallest and hardest (Shannon radii for sixfold coordination in pm: Na 102, Ag 115, K 138, Rb 152, Cs 167).^[41]

The unit cell of the sodium compound **1** is twice as large as that of the silver compound **2**. Conventions for the setting of unit cells make b the stacking vector for **1**, while it is c for **2**. The thickness of the layer packages in both compounds differ only by few percent. The bases of the unit cells that are parallel to the layers are also related: While in **2**, the a and b vectors define a rhombic grid, following the trigonal layer symmetry, the vectors a and c of **1** describe a rectangle, which corresponds to an orthohexagonal setting ($a - c\sqrt{3} = 0.9$ pm), yet without centering. The reflections $h + l = 2n + 1$, which violate the reflection conditions for the B centering and define the larger unit cell for **1**, are much weaker than those with even index sums. In the crystal structure of **1** (Figure 1), the different y coordinates of the Na^+ cations in the same layer interspace are the most obvious deviations from the B centering. If the disordered Ag^+ distribution in **2** is neglected, the structure of **1** can be seen as crystallizing in a *klassengleiche* sub-group of index 2 of the space group of compound **2**.^[42] A representation of the structure of **2** in the "orthohexagonal" setting can be found in the Supporting Information (Figure S2). The positions of the *spiro*-atoms in **1** and **2** (Table S3) deviate only by $\Delta x = 0.014$, $\Delta y = 0.002$, and $\Delta z = -0.020$, supporting the close relation between the two structures.

The hetero *spiro*-dicubane (Bi_7S_8)⁵⁺ (Figure 2) is isomorphous to the cations (Sb_7Se_8)⁵⁺ and (Sb_7Te_8)⁵⁺.^[29–31] It is composed of two (Bi_4S_4)⁴⁺ cubes that share a common bismuth atom vertex. An idealized (Bi_7S_8)⁵⁺ molecule would have the point group symmetry $\bar{3}m$ (D_{3d}). However, the observed crystallographic symmetry is only 1 (C_1), even lower than in $\text{Ag}(\text{Bi}_7\text{S}_8)[\text{S}(\text{AlCl}_3)_3][\text{AlCl}_4]_2$, where the central bismuth atom occupies the 1a Wyckoff position, representing the molecular symmetry $\bar{1}$ (C_1).^[18] While in **2**, the *spiro*-atom is in an almost regular octahedral environment [280.9(4)–281.4(3) pm],^[18] its counterpart in **1** (Bi4) has a [3 + 3] coordination with three shorter [271.5(4)–272.4(4) pm] and three longer [288.2(4)–292.6(4) pm] Bi–S bonds. For the threefold coordinated bismuth atoms the range of Bi–S distances is also broader in **1** [252.5(4)–266.7(3) pm] than in **2** [259.1(3)–267.2(2) pm].^[18] These bismuth atoms are additionally coordinated by chloride ions of the $[\text{AlCl}_4]^-$ and $[\text{S}(\text{AlCl}_3)_3]^{2-}$ groups, with Bi...Cl distances ranging from 304.4(3) to 352.3(3) pm. Bi7 has a distorted octahedral [3S + 3Cl] coordination, while the other bismuth atoms reside in distorted, capped trigonal prisms formed by [3S + 4Cl] (Figure 2). The differences that the interatomic distances of the (Bi_7S_8)⁵⁺ cation show in two comparatively similar compounds demonstrate its sensitivity to the chemical environment. Thus, a detailed comparison to the *spiro*-dicubanes in $M(\text{Sb}_7\text{Te}_8)[\text{TrCl}_4]_6$ ($M = \text{Ag}, \text{Cu}, \text{Na}; \text{Tr} = \text{Al}, \text{Ga}$)^[29–31] appears to be not very instructive.

The Na^+ cation is octahedrally coordinated by six chloride ions that belong to four $[\text{S}(\text{AlCl}_3)_3]^{2-}$ anions and one $[\text{AlCl}_4]^-$

tetrahedron. The Na...Cl distances [280.6(7)–306.0(7) pm] match those observed in $\text{Na}[\text{AlCl}_4]$,^[43] but are longer than in NaCl (281 pm). The displacement ellipsoid of the Na^+ cation is remarkably large, which might be associated with stacking faults (see below).

The two isolated $[\text{AlCl}_4]^-$ tetrahedra show significant differences. The tetrahedron around Al7 is almost regular with bond lengths ranging from 213.0(5) pm to 213.9(5) pm, while the Al8 polyhedron shows four slightly deviating distances between 212.0(5) pm and 215.6(5) pm. All Al–Cl distances are in accordance with those observed in $\text{Na}[\text{AlCl}_4]$ ^[43] and their variation can be correlated with secondary Cl...Bi or Cl...Na bonds.

The anionic group $[\text{S}(\text{AlCl}_3)_3]^{2-}$ consists of three $[\text{AlSCl}_3]^{2-}$ tetrahedra that share their sulfur vertex (Figure 2). All polyhedra point in the same direction. The pseudo-symmetry is 3 m (C_{3v}), while the crystallographic symmetry is only 1 (C_1). Despite the tilting of the tetrahedra, the S–Al bond lengths are rather uniform [226.5(5)–228.2(5) pm]. This anion was first observed in $(\text{Bi}_3\text{S}_4\text{AlCl})[\text{S}(\text{AlCl}_3)_3][\text{AlCl}_4]$.^[17] Most likely a gallium analogue exists in $(\text{Bi}_3\text{GaS}_5)[\text{Ga}_3\text{Cl}_{10}]_2[\text{GaCl}_4]_2\text{S}_8$,^[39] assuming some erroneous assignment of S and Cl, which have very similar scattering factors. Moreover, the selenium compound $(\text{Bi}_4\text{Se}_4)[\text{Se}(\text{GaCl}_3)_3][\text{GaCl}_4]$ exists, which corroborates the atom assignment.^[28]

All investigated crystals of **1** suffered from stacking disorder that caused streaks of diffuse scattering on the reflection rows parallel to b^* . The stacking disorder, or twinning in the case of large domains, is a consequence of the trigonal pseudosymmetry of the layer packages, which permits a rotation of the stacking vector by $\pm 120^\circ$. Because of the translational pseudosymmetry, represented by the above-mentioned group-subgroup relationship, antiphase boundaries can be expected in addition. Although the selected crystal appeared to be relatively unaffected by stacking faults, its real structure manifested itself as unusually high residual electron densities, especially in the immediate vicinity of the bismuth atoms.

3. Conclusions

Lewis-acidic ionic liquids that contain an excess of AlCl_3 proved their ability to activate crystalline Bi_2S_3 at moderate temperatures.

Although the IL is a non-oxidizing solvent, it can replace hot nitric acid, which is commonly used for this purpose. Together with NaCl and the anionic part of the IL, the dissolved Bi_2S_3 forms the complex structured salt $\text{Na}(\text{Bi}_7\text{S}_8)[\text{S}(\text{AlCl}_3)_3][\text{AlCl}_4]_4$. Its layered structure includes cationic *spiro*-dicubanes (Bi_7S_8)⁵⁺ and anionic tetrahedra triples $[\text{S}(\text{AlCl}_3)_3]^{2-}$. Analogous syntheses using the heavier alkali metal ions M^+ ($M = \text{K}, \text{Rb}, \text{Cs}$) yielded compounds of the same kind, whose crystal structures, however, could not be determined because of extensive stacking disorder. The method is not limited to Bi_2S_3 and can also be used to activate other (sulfidic) minerals. Similar ionometallurgical approaches^[44] have the potential to substitute conventional processes, such as roasting of sulfidic ores, which

are associated with high temperatures and the formation of gases with high environmental impact.

Experimental Section

Synthesis: All compounds were handled in an argon-filled glove box (MBraun; $p(\text{O}_2)/p^0 < 1$ ppm, $p(\text{H}_2\text{O})/p^0 < 1$ ppm). The reactions were carried out in silica ampules with a length of 120 mm and a diameter of 14 mm. $\text{Na}(\text{Bi}_7\text{S}_8)[\text{S}(\text{AlCl}_3)_3]_2[\text{AlCl}_4]_2$ was synthesized in the ionic liquid [BMIm]Cl·4AlCl₃, which acted as solvent and reactant. The ampule was loaded with 23.4 mg NaCl (0.4 mmol, 99.98%, Alfa Aesar), 104.0 mg Bi₂S₃ (0.2 mmol, 99.9%, Alfa Aesar), 150.0 mg [BMIm]Cl (0.86 mmol, 98%, Sigma Aldrich, dried under vacuum at 100 °C), and 450.0 mg AlCl₃ (3.38 mmol, sublimed three times). The evacuated and sealed ampule was heated at 180 °C for 6 d and subsequently tilted and cooled to room temperature at $\Delta T/\dot{t} = -6$ K/h⁻¹. The IL was decanted from the precipitated colorless AlCl₃ and the deep red crystals of **1**, which were obtained in sizes of 0.03 to 1 mm. The crystals of **1** were identified visually, according to their color and shape, and separated mechanically from other crystalline species and most of the IL. No further treatment was applied to these crystals, as the small amounts of residual IL on the crystal surface did not impede the following investigations. The excess sodium cations were not detected in any precipitate and are assumed to remain dissolved in the IL. For syntheses with $M = \text{K}$, Rb , Cs , equivalent stoichiometric amounts of $M\text{Cl}$ were used while all other parameters were the same as in the synthesis of **1**. In all three cases, excess metal cations crystallized as ternary $M[\text{AlCl}_4]$ compounds. For $M = \text{Rb}$, crystals of the target composition appeared only as a minor byproduct next to [BMIm](Bi₄S₄)[AlCl₄]₅.

EDX Spectroscopy: EDX measurements were conducted using a SU8020 (Hitachi) SEM equipped with a Silicon Drift Detector (SDD) X-Max^N (Oxford) to check the chemical composition of the crystals. However, several problems impeded the interpretation of the measured data. The [AlCl₄]⁻ ions partially decompose in the high-energetic electron beam ($U_a = 25$ kV) that is necessary to activate bismuth for this measurement.^[45] Considering these factors, we were able to support the composition of $\text{Na}(\text{Bi}_7\text{S}_8)[\text{S}(\text{AlCl}_3)_3]_2[\text{AlCl}_4]_2$ regarding the presence or absence of all elements. Calcd./exp. Na:Bi:S:Al:Cl (at-%) in **1**: 1.9:13.5:19.2:15.4:50/2(1):15(3):11(3):24(2):48(4). For other M , the following experimental ratios were determined: K:Bi:S:Al:Cl (at-%): 1(1):14(2):19(3):18(2):48(6); Rb:Bi:S:A:Cl (at-%): 2(1):15(2):17(3):21(2):47(5); Cs:Bi:S:Al:Cl (at-%): 2(1):13(2):13(3):23(2):49(4).

Powder X-ray Diffraction: Data collection was performed at 296(2) K with an X'Pert Pro MPD diffractometer (PANalytical) equipped with a Ge(220) hybrid-monochromator using Cu-K_{α1} radiation ($\lambda = 154.056$ pm). Due to their sensitivity to moisture, the samples were contained in a glass capillary (Hilgenberg) with an outer diameter of 0.3 mm. A Le Bail fit was conducted for the lattice parameters of $\text{Na}(\text{Bi}_7\text{S}_8)[\text{S}(\text{AlCl}_3)_3]_2[\text{AlCl}_4]_2$ based on the values gathered in the SCXRD measurements at 100(2) K with TOPAS.^[46]

X-ray Crystal Structure Determination: Single-crystal X-ray diffraction was measured on a four-circle Kappa APEX II CCD diffractometer (Bruker) with a graphite(002)-monochromator and a CCD-detector at $T = 100(2)$ K. Mo-K_α radiation ($\lambda = 71.073$ pm) was used. The datasets were corrected for background, polarization and Lorentz factor using the APEX3 software suite.^[47] After integration,^[47] a numerical absorption correction based on an optimized crystal description was applied.^[48] The initial structure solution was performed with JANA2006^[49] and further refinement processed in SHELXL against F_o^2 .^[50–52] The unit cell setting was

chosen so that (a) all angles are smaller than 90° and (b) one face of the cell is parallel to the layer packages in the structure, which also simplifies the group-subgroup relationship to the silver compound.

$\text{Na}(\text{Bi}_7\text{S}_8)[\text{S}(\text{AlCl}_3)_3]_2[\text{AlCl}_4]_2$: triclinic; $P\bar{1}$ (no. 2); $T = 100(2)$ K; $a = 1846.4(1)$ pm, $b = 1905.1(2)$ pm, $c = 1065.5(2)$ pm, $\alpha = 84.07(1)^\circ$, $\beta = 89.55(1)^\circ$, $\gamma = 49.68(1)^\circ$; $V = 2883.9(4) \times 10^6$ pm³; $Z = 2$; $\rho_{\text{calcd.}} = 3.450$ g cm⁻³; $\mu(\text{Mo-K}_\alpha) = 23.4$ mm⁻¹; $2\theta_{\text{max}} = 54.0^\circ$, $-23 \leq h \leq 23$, $-24 \leq k \leq 24$, $-13 \leq l \leq 13$; 61896 measured, 12231 unique reflections, $R_{\text{int}} = 0.087$, $R_\sigma = 0.098$; 469 parameters, $R_1[\sum w(F_o - F_c)^2] = 0.046$, $wR_2[\sum w(F_o^2 - F_c^2)^2] = 0.071$, $\text{Goof} = 1.095$, min./max. residual electron density: $-3.87/5.67 \text{ e} \times 10^{-6} \text{ pm}^{-3}$. For atomic parameters see Table S2 of the Supporting Information.

Further details of the crystal structure determination are available from the Fachinformationszentrum Karlsruhe, D-76344 Eggenstein-Leopoldshafen (Germany), E-mail: crysdata@fiz-karlsruhe.de, on quoting the depository number CSD-2090776 for $\text{Na}(\text{Bi}_7\text{S}_8)[\text{S}(\text{AlCl}_3)_3]_2[\text{AlCl}_4]_2$.

Acknowledgements

This work was financially supported by the Deutsche Forschungsgemeinschaft (DFG) within the priority program SPP 1708. We acknowledge technical support by H. Poddig, A. Brünner and M. Münch.

Conflict of Interest

The authors declare no conflict of interest.

Keywords: bismuth · heterocubanes · ionic liquids · ionothermal synthesis · spirocubanes

- [1] P. Wasserscheid, T. Welton, *Ionic Liquids in Synthesis*, Wiley, 2008.
- [2] D. Freudenmann, S. Wolf, M. Wolff, C. Feldmann, *Angew. Chem.* **2011**, *123*, 11244–11255; *Angew. Chem. Int. Ed.* **2011**, *50*, 11050–11060.
- [3] X. Duan, J. Ma, J. Lian, W. Zheng, *CrystEngComm* **2014**, *16*, 2550–2559.
- [4] X. Kang, X. Sun, B. Han, *Adv. Mater.* **2016**, *28*, 1011–1030.
- [5] Z. Ma, J. Yu, S. Dai, *Adv. Mater.* **2010**, *22*, 261–285.
- [6] S. Santner, J. Heine, S. Dehnen, *Angew. Chem.* **2016**, *128*, 886–904; *Angew. Chem. Int. Ed.* **2016**, *55*, 876–893.
- [7] E. Ahmed, J. Breternitz, M. F. Groh, M. Ruck, *CrystEngComm* **2012**, *14*, 4874–4885.
- [8] M. F. Groh, U. Müller, E. Ahmed, A. Rothenberger, M. Ruck, *Z. Naturforsch. B* **2014**, *68*, 1108–1122.
- [9] J. Estager, J. D. Holbrey, M. Swadzba-Kwasny, *Chem. Soc. Rev.* **2014**, *43*, 847–886.
- [10] M. F. Groh, A. Wolff, M. A. Grasser, M. Ruck, *Int. J. Mol. Sci.* **2016**, *17*, 1452.
- [11] M. Antonietti, D. Kuang, B. Smarsly, Y. Zhou, *Angew. Chem.* **2004**, *116*, 5096–5100; *Angew. Chem. Int. Ed.* **2004**, *43*, 4988–4992.
- [12] A. Wolff, T. Doert, J. Hunger, M. Kaiser, J. Pallmann, R. Reinhold, S. Yogendra, L. Giebeler, J. Sichelschmidt, W. Schnelle, R. Whiteside, H. Q. N. Gunaratne, P. Nockemann, J. J. Weigand, E. Brunner, M. Ruck, *Chem. Mater.* **2018**, *30*, 7111–7123.
- [13] E. Ahmed, M. Ruck, *Coord. Chem. Rev.* **2011**, *255*, 2892–2903.
- [14] J. Richter, M. Ruck, *Molecules* **2020**, *25*, 78.
- [15] J. Richter, M. Ruck, *RSC Adv.* **2019**, *9*, 29699–29710.
- [16] M. F. Groh, M. Knies, A. Isaeva, M. Ruck, *Z. Anorg. Allg. Chem.* **2015**, *641*, 279–284.

- [17] M. F. Groh, A. Isaeva, U. Müller, P. Gebauer, M. Knies, M. Ruck, *Eur. J. Inorg. Chem.* **2016**, *6*, 880–889.
- [18] M. Knies, M. F. Groh, T. Pietsch, M. Lê Anh, M. Ruck, *ChemistryOpen* **2021**, *10*, 110–116.
- [19] T. Zhang, K. Schwedtmann, J. J. Weigand, T. Doert, M. Ruck, *Chem. Eur. J.* **2018**, *24*, 9325–9332.
- [20] S. Sowmiah, V. Srinivasadesikan, M.-C. Tseng, Y.-H. Chu, *Molecules* **2009**, *14*, 3780–3813.
- [21] T. Zhang, T. Doert, H. Wang, S. Zhang, M. Ruck, *Angew. Chem.* DOI: 10.1002/ange.202104035; *Angew. Chem. Int. Ed.* DOI: 10.1002/anie.202104035
- [22] R. J. Gillespie, P. R. Ireland, J. E. Vekris, *Can. J. Chem.* **1975**, *53*, 3147–3152.
- [23] R. J. Gillespie, D. R. Slim, J. D. Tyrer, *J. Chem. Soc. Chem. Commun.* **1977**, 253–255.
- [24] R. J. Gillespie, J. P. Kent, J. F. Sawyer, *Inorg. Chem.* **1981**, *20*, 3784–3799.
- [25] K.-O. Feldmann, T. Wiegand, J. Ren, H. Eckert, J. Breternitz, M. F. Groh, U. Müller, M. Ruck, B. Maryasin, C. Ochsenfeld, O. Schön, K. Karaghiosoff, J. J. Weigand, *Chem. Eur. J.* **2015**, *21*, 9697–9712.
- [26] B. H. Christian, R. J. Gillespie, J. F. Sawyer, *Inorg. Chem.* **1981**, *20*, 3410–3420.
- [27] J. Beck, S. Schlüter, N. Zotov, *Z. Anorg. Allg. Chem.* **2005**, *631*, 2450–2456.
- [28] A. Eich, *PhD thesis*, Rheinische Friedrich-Wilhelms-Universität Bonn, **2015**.
- [29] A. Eich, S. Schlüter, G. Schnakenburg, J. Beck, *Z. Anorg. Allg. Chem.* **2013**, *639*, 375–383.
- [30] A. Eich, W. Hoffbauer, G. Schnakenburg, T. Bredow, J. Daniels, J. Beck, *Eur. J. Inorg. Chem.* **2014**, *2014*, 3043–3052.
- [31] A. Eich, J. Beck, *Z. Anorg. Allg. Chem.* **2014**, *640*, 2788–2791.
- [32] E. Ahmed, J. Breternitz, M. F. Groh, A. Isaeva, M. Ruck, *Eur. J. Inorg. Chem.* **2014**, *2014*, 3037–3042.
- [33] Q. Zhang, I. Chung, J. I. Jang, J. B. Ketterson, M. G. Kanatzidis, *J. Am. Chem. Soc.* **2009**, *131*, 9896–9897.
- [34] E. Ahmed, A. Isaeva, A. Fiedler, M. Haft, M. Ruck, *Chem. Eur. J.* **2011**, *17*, 6847–6852.
- [35] J. Beck, S. Schlüter, *Z. Anorg. Allg. Chem.* **2005**, *631*, 569–574.
- [36] M. F. Groh, J. Breternitz, E. Ahmed, A. Isaeva, A. Efimova, P. Schmidt, M. Ruck, *Z. Anorg. Allg. Chem.* **2015**, *641*, 388–393.
- [37] J. Beck, S. Schlüter, N. Zotov, *Z. Anorg. Allg. Chem.* **2004**, *630*, 2512–2519.
- [38] J. Beck, M. Dolg, S. Schlüter, *Angew. Chem.* **2001**, *113*, 2347–2350; *Angew. Chem. Int. Ed.* **2001**, *40*, 2287–2290.
- [39] D. Freudenmann, C. Feldmann, *Dalton Trans.* **2010**, *40*, 452–456.
- [40] V. Kopský, D. B. Litvin, *International Tables for Crystallography. Volume E, Subperiodic Groups*, Kluwer Academic Publishers, London, **2002**.
- [41] R. D. Shannon, *Acta Crystallogr. Sect. A* **1976**, *32*, 751–767.
- [42] U. Müller, *Symmetry Relationships between Crystal Structures: Applications of Crystallographic Group Theory in Crystal Chemistry*, Oxford University Press, **2013**.
- [43] N. C. Baenziger, *Acta Crystallogr.* **1951**, *4*, 216–219.
- [44] J. Richter, M. Knies, M. Ruck, *ChemistryOpen* **2021**, *10*, 97–109.
- [45] U. Müller, A. Isaeva, J. Richter, M. Knies, M. Ruck, *Eur. J. Inorg. Chem.* **2016**, *2016*, 3580–3584.
- [46] A. Coelho, *TOPAS-Academic V5*, Brisbane, Australia, **2012**.
- [47] Bruker, *APEX3 Suite for Crystallographic Software*, Bruker AXS Inc., Madison, Wisconsin, USA, **2017**.
- [48] X-Shape, Crystal Optimization for Numerical Absorption Correction Program, Stoe & Cie GmbH, Darmstadt, Germany, **2008**.
- [49] V. Petricek, M. Dusek, L. Palatinus, *JANA2006, The Crystallographic Computing System*, Institute of Physics, Praha, Czech Republic, **2011**.
- [50] G. M. Sheldrick, *Acta Crystallogr. Sect. A* **2008**, *64*, 112–122.
- [51] G. M. Sheldrick, *SHELXL, Program for Crystal Structure Refinement – Multi-CPU*, Georg-August-Universität Göttingen, Göttingen, Germany, **2014**.
- [52] G. M. Sheldrick, *Acta Crystallogr. Sect. C* **2015**, *71*, 3–8.

Manuscript received: June 18, 2021

Revised manuscript received: July 30, 2021